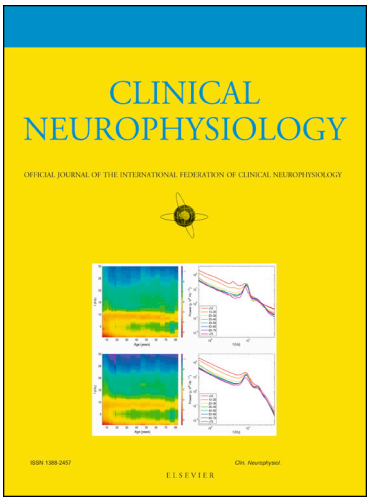

Revisiting interhemispheric imbalance in chronic stroke: a tDCS study

Alana B McCambridge, James W Stinear, Winston D Byblow

PII: S1388-2457(17)31108-2
DOI: https://doi.org/10.1016/j.clinph.2017.10.016
Reference: CLINPH 2008306

To appear in: *Clinical Neurophysiology*

Accepted Date: 1 October 2017

Please cite this article as: McCambridge, A.B., Stinear, J.W., Byblow, W.D., Revisiting interhemispheric imbalance in chronic stroke: a tDCS study, *Clinical Neurophysiology* (2017), doi: https://doi.org/10.1016/j.clinph.2017.10.016

Revisiting interhemispheric imbalance in chronic stroke: a tDCS study

Alana B McCambridge, PhD [1,2,3], James W Stinear, PhD [1,2], Winston D Byblow, PhD [1,2]

[1] Department of Exercise Sciences, University of Auckland, New Zealand

[2] Centre for Brain Research, University of Auckland, New Zealand

[3] Graduate School of Health, University of Technology Sydney, Australia

Corresponding author:

Winston D Byblow

Professor of Neuroscience

Director, Movement Neuroscience Laboratory

Department of Exercise Sciences, Centre for Brain Research

The University of Auckland, New Zealand

Tel.: +64 9 923 6844

E-mail: w.byblow@auckland.ac.nz

Keywords: Contralesional, transcranial direct current stimulation, tDCS, stroke, transcranial magnetic stimulation, TMS, magnetic resonance imaging, magnetic resonance spectroscopy, interhemispheric competition.

Highlights

- Our findings contradict a strict inter-hemispheric competition model after chronic stroke.
- The contralesional primary motor cortex (M1) is a feasible target for anodal transcranial direct current stimulation (tDCS) in moderate to severely impaired patients.
- Anodal tDCS of contralesional M1 facilitated contralesional and ipsilesional corticomotor excitability.

Abstract

Objective: Chronic stroke patients with moderate-severe motor impairment may have an increased reliance on contralesional vs ipsilesional motor areas to control the paretic arm. We hypothesised that increasing contralesional excitability with anodal transcranial direct current stimulation (a-tDCS) would benefit motor performance in patients with moderate-severe impairment.

Methods: Ten patients with motor impairment at the chronic stage after stroke received a-tDCS, cathodal (c-tDCS) and sham with the target electrode over contralesional motor cortex (M1). Motor performance was quantified from the circularity and size of planar movements made with the paretic arm. Contralateral and ipsilateral corticospinal excitability was inferred using transcranial magnetic stimulation. Corticospinal tract integrity and basal GABA concentration were assessed with magnetic resonance imaging and spectroscopy.

Results: Anodal tDCS increased contralesional corticomotor excitability evident from motor evoked potentials in both wrist extensors (both $P<0.043$). Cathodal tDCS did not affect corticomotor excitability ($P>0.37$). The effect of tDCS on motor performance with the paretic limb was negatively associated with ipsilesional GABA concentration after c-tDCS ($P=0.001$).

Conclusions: Further investigation of noninvasive brain stimulation protocols that facilitate contralesional M1 is warranted.

Significance: The inter-hemispheric imbalance model of stroke recovery may not apply to patients with more severe impairment.

1.1 Introduction

The immense burden of stroke-related disability has led to the development of noninvasive brain stimulation (NIBS) as a possible approach to augment neurorehabilitation of the paretic upper limb (Ackerley et al., 2010). Transcranial direct current stimulation (tDCS) is a polarity-dependent neuromodulatory technique that has demonstrated some benefit to motor function at the chronic stage (>6 months) post stroke, but effect sizes have varied (Jacobson et al., 2012, Kang et al., 2015).

A prevailing model of interhemispheric imbalance after stroke espouses that NIBS be used to up-regulate excitability in ipsilesional motor cortex (M1) and down-regulate excitability in the contralesional M1 (Nowak et al., 2009). However, recent reviews suggest the interhemispheric imbalance model may be too simplistic, and instead advocate for multi-dimensional models that take into account the extent of structural damage and availability of residual motor pathways (Bradnam et al., 2013, Di Pino et al., 2014, Plow et al., 2016). Multimodal imaging studies have demonstrated increased task-related contralesional brain activation, even in well-recovered patients (Ward et al., 2003, Gerloff et al., 2006, Lotze et al., 2006, Lotze et al., 2012), and disruptive TMS applied to contralesional networks has led to performance decrements in tasks performed with the paretic hand (Johansen-Berg et al., 2002, Lotze et al., 2006). Contralesional motor network activation appears to scale with the extent of damage to the ipsilesional corticospinal pathway (Lotze et al., 2012). Therefore reliance on the contralesional motor network should be taken into consideration when delivering NIBS. For example, in two studies of moderate-to-severely impaired chronic stroke patients, contralesional cathodal tDCS (c-tDCS) degraded motor performance of the paretic upper limb (Bradnam et al., 2012, Yao et al., 2015). Degradation was possibly due to the suppressive effect of c-tDCS on ipsilateral motor pathways e.g., cortico-reticulo-

propriospinal projections from the contralesional M1 (Bradnam et al., 2013). The aforementioned studies support a growing body of evidence that suggests when impairment is more severe, there is greater up-regulation of the contralesional M1 which may represent adaptation that is functionally important for control of the paretic upper limb (see reviews Bradnam et al. (2013), Di Pino et al. (2014), Jones et al. (2015)). For these reasons, tDCS approaches based on interhemispheric imbalance alone may not be suitable for all patients.

The primary aim of this study was to investigate whether patients with moderate-to-severe upper limb impairment at the chronic stage after stroke would benefit from tDCS which aims to increase excitability of contralesional M1. We recruited patients across a range of impairment levels and the effect of a single session of contralesional anodal tDCS (a-tDCS) and c-tDCS were compared to sham stimulation. We examined intralimb coordination of the upper limb with a circle drawing task requiring proximal-distal motor control. Coordination of proximal and distal musculature is essential for functional movements with the upper limb. Circle drawing metrics have been used to investigate abnormal synergistic movement patterns that can develop after stroke (Dipietro et al., 2007, Krabben et al., 2011a, Krabben et al., 2011b). The neurophysiological after-effects of tDCS were examined using transcranial magnetic stimulation (TMS) and peripheral nerve stimulation. TMS was used to examine the effects of tDCS on contralateral and ipsilateral corticomotor excitability. Peripheral nerve stimulation was used to probe cervical propriospinal excitability (Mazevet et al., 2003), as tDCS was expected to alter excitability along the cortico-reticulo-propriospinal pathway as demonstrated previously (Bradnam et al., 2011, McCambridge et al., 2014). We hypothesised that tDCS would modulate corticomotor excitability and motor function in a polarity dependent manner, whereby a-tDCS may increase corticomotor excitability and improve intralimb coordination, whereas c-tDCS may decrease corticomotor excitability and degrade intralimb coordination. Our secondary aim was to determine potential biomarkers for

individualising tDCS from clinical, neurophysiological or magnetic resonance imaging (MRI) and spectroscopy (MRS) measures.

2.1 Methods

2.1.1 Participants

Ten chronic stroke patients met the study criteria (Table 1). Patients were included if they were >6 months post stroke, had upper limb impairment (Upper Limb Fugl-Meyer (UL-FM) score ≤58) and spasticity (modified Ashworth spasticity (MAS) ≥1). Participants were excluded if they had contraindications to TMS or MRI. Written informed consent was provided and the study approved by the regional ethics committee.

2.1.2 Study protocol

The study protocol is outlined in Figure 1. Participants attended an initial screening session where they were tested on the UL-FM, action research arm test (ARAT), and MAS at the elbow by a therapist that took no part in the following sessions or analysis. Participants that met the study criteria attended 3 experimental sessions, receiving a-tDCS, c-tDCS or sham-tDCS in separate sessions. The intervention was double-blinded and session order randomised. On a separate day, participants underwent MRI of their brain.

2.1.3 Electromyography

Surface electromyography (EMG) was recorded from left and right *biceps brachii* (BB) and *extensor carpi radialis* (ECR) using disposable electrodes (Ambu Blue Sensor Paediatric NS, Ballerup) placed over the muscle bellies. EMG signals were amplified (CED 1902, Cambridge), band-passed filtered (2–1,000 Hz), and sampled at 2 kHz (CED 1401, Cambridge). EMG data were analysed using Signal software v4.11 (CED, Cambridge).

2.1.4 Transcranial magnetic stimulation

Single-pulse TMS was delivered to M1 with a figure-of-eight MC-B70 coil using a MagPro X100 +Option (MagVenture, Farum). The current was directed posterior-to-anterior across the central sulcus and the optimal site for eliciting contralateral MEPs (cMEP) was marked on the scalp. If MEPs were not evident in the paretic upper limb at maximum stimulator output (MSO) the participant was deemed MEP negative. The rest motor threshold (RMT) was defined as the minimum intensity that evoked a 50 μV cMEP in four out of eight trials. The stimulation intensity was 130% RMT. Sixteen stimuli were delivered at each time point.

To evoke ipsilateral MEPs (iMEP) in the paretic BB, the TMS coil was positioned over the contralesional M1. The stimulation intensity was 100% MSO. Participants were asked to perform an isometric unilateral elbow flexion contraction with their paretic upper limb at 50% maximum voluntary contraction (MVC). Sixteen stimuli were delivered and rest breaks were given after every stimulus to avoid fatigue.

2.1.5 Peripheral nerve stimulation

A Digitimer DS7A constant current stimulator delivered electrical pulses to the left and right superficial radial nerves via adhesive electrodes placed on medial and lateral aspects of the wrist. The superficial radial nerve was located by moving a custom stimulating clip around the wrist until a single square wave pulse (1 ms, 300 V) produced radiating sensation in the dorsal side of the hand or first three fingers. Stimulation intensity was 3 × perceptual threshold (PT) and delivered as a train of stimulation (3 pulses at 300 Hz). For one participant, the stimulation intensity was deemed painful and was decreased to 1.5 × PT.

Participants were asked to activate their ECR by lifting their arm against gravity to an elbow angle of 145°, wrists neutral. EMG was continuously monitored online by the

experimenter and verbal feedback given. Conditioned trials (C) included peripheral nerve stimulation and non-conditioned trials (NC) had no stimulation. Trials were randomly delivered in a 15 second block with rest periods between. Participants who could not voluntarily extend their paretic wrist by at least 10° were excluded (Mazevet et al., 2003). A total of 210 trials were recorded on the non-paretic side, and 150–210 trials on the paretic side.

2.1.6 Circling task

Participants were seated in front of a touch screen (PQ labs, California) laid horizontal on a surface. A template circle (14 cm radius) was displayed on the wall facing the participants. If a participant could not extend a finger to make contact with the touch screen, a stylus was strapped inside their paretic hand. The task instructions were to draw 5 continuous circles as similar as possible to the template. Four trials were performed with the experimenter instructing participants to start at the leftmost or rightmost side and to draw clockwise or anti-clockwise. The x-y coordinates were sampled at 100 Hz and stored to disk for offline analysis.

2.1.7 Transcranial direct current stimulation

HDCstim direct current stimulators (Newronika) delivered tDCS via a dedicated tDCS electrode cap (MindCap, Newronika) with 20 cm^2 oval sponge electrodes soaked in saline. An unblinded experimenter programmed the tDCS units and positioned the electrode cap but took no part in data collection or analysis. For each montage, the target electrode was positioned over contralesional M1 and the 'reference' over the contralateral forehead. For real and sham stimulation, current was ramped up to 1 mA over 7 seconds and ramped down to 0 mA over 7 seconds. Real tDCS duration was 15 minutes. Sham tDCS stimulation duration was 36 seconds. Participants were instructed to sit quietly throughout stimulation

until the circle drawing task was initiated after 10 min of stimulation. The time between the onset of tDCS and commencement of circle drawing ensured the participants were comfortable with the stimulation prior to task activity.

2.1.8 Magnetic resonance imaging and spectroscopy

All images were acquired using a Siemens Skyra 3T scanner. A high-resolution T1-weighted anatomical image (Figure 2) was acquired (repetition time, TR=1.9 s; echo time, TE=2.07 ms, field of view, FOV=256 mm, voxel dimensions=1 mm^3). Diffusion-weighted imaging (DWI) was performed with a single-shot echo planar imaging sequence (TR=3.6 s, TE=92.4 ms, FOV=220 mm, voxel=2 mm^3), with diffusion gradients along 30 directions (b=2000 s/mm^2). Single-voxel spectroscopy data were acquired for ipsilesional and contralesional M1, and contralesional visual cortex (V1). The voxel of interest (18 mm^3) was positioned using anatomical landmarks from each participant's T1-weighted image. The left and right precentral gyrus was identified and the voxel for ipsilesional and contralesional M1 positioned over the hand knob (Yousry et al., 1997). The V1 voxel was positioned on the medial aspect of the contralesional hemisphere in the posterior portion of the occipital lobe. To assess creatine (Cr) linewidths, a PRESS sequence (TR=1.5 s, TE=68 ms, 96 averages) was used to acquire an unedited spectrum. Finally, a MEGA-PRESS sequence (TR=1.5 s, TE=68 ms, 96 averages) was used for simultaneous spectral gamma-amino butyric acid (GABA) editing and water suppression (Mescher et al., 1998).

2.2 Data processing and analysis

2.2.1 Aspect ratio

The spatial performance of each hand was determined by fitting each closed trajectory (circle) to a best-fitting ellipse (Walters et al., 1997). The aspect ratio (AR) was calculated by expressing the primary and secondary axes of the ellipse as a ratio (AR=secondary/primary).

The AR provides a measure of circularity, such that a ratio of 1 resembles a perfect circle. The AR was log-transformed for analysis (Mardia et al., 1975) and delta AR was calculated between real and sham for each time point (ΔAR=real–sham). As there was no prior hypothesis regarding time, a combined ΔAR was calculated as the average between post 1 and 2 ($\Delta AR_{1\&2}$).

2.2.2 Contralateral MEP

In both ECR, cMEP areas were calculated from the integral of the rectified EMG within a 20 ms window from the MEP onset. The root mean square of the pre-trigger EMG (rmsEMG) was measured prior to stimulus artefact and traces with >12 μV rmsEMG were rejected from analysis. To examine the effects of tDCS on cMEPs, cMEP area was expressed as a ratio from pre tDCS cMEP area (i.e., post/pre). There was no hypothesis regarding time, therefore cMEP ratio at $post_1$ and $post_2$ was averaged across time ($cMEP_{1\&2}$).

2.2.3 Ipsilateral MEP

Ipsilateral MEPs were identified from the rectified EMG traces of the paretic BB (Ziemann et al., 1999). The earliest iMEP onset and latest iMEP offset across all sessions was identified as the iMEP window for each individual. The iMEP area was calculated as the integral of rectified EMG within the iMEP window less an equivalent window of background EMG. To examine the effects of tDCS, iMEPs after real tDCS were expressed relative to sham (iMEP ratio=real/sham). The iMEP persistence was measured as the percentage of iMEPs >0.1 mV·ms out of the total number of stimuli.

2.2.4 EMG suppression

The early propriospinal component and late cortical component was measured from the rectified EMG for the early component 26–36 ms after the last stimulus and 41–51 ms for

the late component. The time windows for each component were based on a previous study (see Mazevet et al. (2003) for details). EMG suppression (%) for the early and late component was calculated as ((1 – (C/NC)) x 100).

2.2.5 Fractional anisotropy asymmetry index

Diffusion image processing was carried out with FSL/FDT (Diffusion toolbox, FMRIB Software Library, Oxford). Diffusion weighted images were skull stripped using the brain extraction tool (BET) (Smith, 2002) and corrected for motion and eddy currents. The mean fractional anisotropy (FA) was calculated within the posterior limbs of the internal capsules (PLIC) to quantify the integrity of the ipsilesional CST (FA_{Ipsi}) and contralesional CST (FA_{Contra}). An FA asymmetry index (FA_{AI}) was calculated as $FA_{AI} = (FA_{Contra} – FA_{Ipsi}) / (FA_{Contra} + FA_{Ipsi})$. This yields a value between -1 and +1 for each participant. Positive values correspond to reduced FA in the ipsilesional PLIC.

2.2.6 GABA concentration

MRS data were first processed using jMRUI v5.1. Data were corrected for non-zero DC offset, smoothed using 2 Hz Lorentzian filter, and phase corrected. The residual water signal was removed using a Hankel Lanczos singular value decomposition (HLSVD) filter. Creatine (Cr) line-widths were obtained from the non-edited PRESS using the non-linear least square fitting algorithm (AMARES) and were used to constrain the GABA linewidth from the edited spectrum (Vanhamme et al., 2001). The GABA optimised spectra were then pre-processed and analysed using AMARES, as above. Gaussian curves were used to fit all resonances.

FMRIB's Automated Segmentation Tool (FAST) (Zhang et al., 2001) was used to calculate the relative quantities of grey matter (GM), white matter (WM) and cerebral spinal fluid (CSF) in each voxel from the T1-weighted structural image. The amplitude of the Cr

peak was corrected for the proportion of total brain tissue volume within the voxel by applying a multiplication factor ([GM + WM] / [GM + WM + CSF]). The amplitude of the GABA peak was corrected for the proportion of GM volume with the voxel by applying a multiplication factor ([GM] / [GM + WM + CSF]) (Stagg et al., 2011a). The corrected quantities of GABA and Cr within each voxel were expressed as a ratio, GABA:Cr.

2.2.7 Statistical Analyses

Statistical analyses were conducted using non-parametric tests due to the small sample size (SPSSv.22, IBM Corp). To determine effects on corticomotor excitability and circling performance, one-sample signed rank tests were used to detect changes from baseline. Wilcoxon related-samples signed rank tests were used to compare the after-effects of anodal or cathodal tDCS to sham tDCS. To confirm RMT and rmsEMG were comparable across sessions and time, a Friedman test was used for each arm separately. Spearman's rho correlations were used to investigate known associations between upper limb impairment and circle drawing performance, and upper limb impairment and FAAI at the PLIC. Spearman's rho correlations were conducted to identify variables that may determine the overall effect of anodal or cathodal tDCS on upper limb coordination. The variables tested were UL-FM, ARAT, MAS, FA asymmetry index (FA_{AI}), baseline AR, time post stroke, ipsilesional GABA:Cr and contralesional GABA:Cr. These variables have previously been shown to determine tDCS after-effects at the chronic stage post stroke (Bradnam et al., 2012, O'Shea et al., 2014). Effects were deemed significant if $P<0.05$ and a trend was recognised if $P=0.05$-0.10. Median (25^{th} percentile, 75^{th} percentile) are reported in the text unless otherwise stated.

3.1 Results

None of the participants experienced any adverse events to the procedures.

3.1.1 Contralateral MEPs in non-paretic and paretic ECR

In the non-paretic ECR, the combined cMEP ratio ($cMEP_{1\&2}$), revealed a-tDCS facilitated cMEPs (z=2.19, *P*=0.028) and cMEP area after a-tDCS differed from sham (z=-2.19, *P*=0.028; Figure 3A). In contrast, $cMEP_{1\&2}$ after c-tDCS and sham was neither facilitated nor suppressed (both *P*>0.374), and did not differ between c-tDCS and sham sessions (z=-1.58, *P*=0.114). Analysis of each time point separately revealed at $post_1$ there was a non-significant trend for non-paretic ECR cMEP area to be facilitated after a-tDCS (a-$tDCS_{post1}$=1.39 (0.78, 1.73), z=1.89, *P*=0.059), and suppressed after sham ($sham_{post1}$0.82 (0.59, 0.99), z=-1.79, *P*=0.074). At $post_1$, ECR cMEP after a-tDCS (z=-1.99, *P*=0.037), and c-tDCS was different to sham (c-$tDCS_{post1}$=1.1 (0.89, 1.77); z=-1.99 , *P*=0.047). At $post_2$, ECR cMEP area was facilitated after a-tDCS (a-$tDCS_{post2}$=1.7 (1.03, 1.89); z=2.29, *P*=0.022) and differed from sham ($sham_{post2}$=1.04 (0.90, 1.25; z=-0.92, *P*=0.047).

Paretic cMEPs were able to be evoked in 6 participants, and the participants without cMEPs on the paretic side were the most impaired (Figure 4A). Relative to sham, cMEP area was greater in the paretic ECR after a-tDCS (z=-2.02, *P*=0.043) and there were no differences in paretic cMEPs after c-tDCS (z=-1.36, *P*=0.173; Figure 3B). One-sample signed rank tests did not reveal MEP facilitation or suppression on the paretic side (all *P*>0.249). The paretic cMEP latency was longer than the non-paretic cMEP latency (21.63 (20.60, 22.65) ms vs 17.78 (16.89, 18.47) ms; z=-3.72, *P*<0.001).The median RMT was 44% MSO for the paretic ECR and 48 % MSO for the non-paretic ECR. RMT and rmsEMG for the paretic and non-paretic sides did not differ between sessions (all *P*>0.225).

3.1.2 Ipsilateral MEPs in Paretic BB

In the paretic BB, iMEPs were observed in 8 participants (iMEP latency 19.72 (17.88, 22.16) ms). The persistence of iMEPs was 89.5% (80.8%, 93.7%) after a-tDCS, 72.0%

(53.8%, 94.0%) after c-tDCS, and 72.0% (55.5%, 93.3%) after sham (both P>0.139. Due to the high variability of iMEPs, iMEP area during real tDCS sessions was expressed as a ratio to sham. The iMEP ratio after a-tDCS revealed a trend towards iMEP facilitation (z = 1.82, P=0.069) and the iMEP ratio after c-tDCS remained unchanged (z = 0.98,P=0.327; Figure 3C).

3.1.3 Propriospinal-mediated EMG Suppression

Cutaneous-induced suppression in the paretic ECR was observed in 4 participants who could voluntarily extend their paretic wrist. Therefore analyses of the paretic ECR are under-powered and should be interpreted cautiously. One-sample signed rank tests revealed cutaneous-induced suppression of the EMG for the early and late component was present in all sessions for the non-paretic arm (all P<0.005). For the paretic arm, there was a trend towards suppression after a-tDCS in the early and late component (both P=0.068, n=4) and after sham in the late component only (z=1.83, P=0.068). EMG suppression after sham was 13.0% and 19.0% for the early component in the non-paretic and paretic arm respectively, and 33.5% and 24.5% for the late component (Figure 3D-E). For the non-paretic arm there were no differences between real and sham tDCS for either component (all P>0.139, Figure 3D). For the paretic arm, the late component showed a trend for less suppression after a-tDCS compared to sham (z=-1.83, P=0.068, all others P>0.715, Figure 3E).

3.1.4 Upper limb aspect ratios

As expected, circles traced with the paretic side were smaller and less circular than those made with the non-paretic side. The non-transformed aspect ratios were 0.82 (0.76, 0.86) with the non-paretic arm and 0.60 (0.37, 0.79) with the paretic arm. The size of circles drawn with the paretic arm was 53% of the size of those drawn with the non-paretic arm remained consistent between session and time-points (all P>0.148). There was a trend for a-

tDCS to improve ΔAR in the paretic arm at $post_1$ (z=1.89, *P*=0.059) but not $post_2$ (z=0.97, *P*=0.330; Figure 5A). Cathodal tDCS did not modulate ΔAR in the paretic arm at $post_1$ or $post_2$ (both *P*>0.767; Figure 5A). The combined ΔAR did not reveal any differences after a-tDCS or c-tDCS sessions (both *P*>0.126; Figure 5A). There were no effects of tDCS on ΔAR with the non-paretic arm (all *P*>0.201).

3.1.5 GABA concentration

GABA:Cr ratios were 0.09 (0.07, 0.13) in the ipsilesional M1, 0.12 (0.09, 0.19) in the contralesional M1, and 0.10 (0.07, 0.12) in the contralesional V1. GABA:Cr did not differ between each M1 and V1 (both *P*>0.114) or between contralesional and ipsilesional M1 (z=-1.58, *P*=0.114). One participant had a negligible amount of tissue within the ipsilesional voxel due to the extent of stroke-related damage, therefore analyses were repeated with this case excluded and no differences were detected (both *P*>0.173).

3.1.6 Correlation and Regression Analyses

Posterior limb of the internal capsule FA_{AI} measures are shown in Table 1. There was a negative correlation between FA_{AI} and UL-FM score (ρ=-0.65, *P*=0.043; Figure 4A). Patients with more severe impairment had the greatest asymmetry, and those with FA_{AI} >0.3 were MEP negative (Figure 4A). Aspect ratios obtained in the sham tDCS session were strongly correlated with UL-FM and ARAT (both ρ>0.67, *P*<0.036; Figure 4B-C), confirming that the circle drawing task was a useful surrogate measure of upper limb function.

Ipsilesional GABA concentration was negatively associated with $\Delta AR_{1\&2}$ after c-tDCS (ρ =0.87,*P*=0.001,Figure 5C) such that movement circularity tended to worsen in patients with higher concentrations of ipsilesional GABA. After a-tDCS, there was a trend for MAS score to be positively associated with $\Delta AR_{1\&2}$ (ρ=0.63, *P*=0.052; Figure 5B). The circle

drawing movements tended to improve the most in patients with higher levels of spasticity. For both a-tDCS and c-tDCS sessions, the effect of tDCS on circle drawing performance was not correlated to the modulation of cMEPs or iMEPs in the paretic arm (all $P > 0.208$).

4.1 Discussion

In a small heterogeneous sample of chronic stroke patients, a-tDCS over the contralesional M1 increased corticomotor excitability of both hemispheres, and there was a trend toward improved paretic intralimb coordination. Cathodal-tDCS had no effect on contralesional M1 excitability or motor function. These findings contradict a model of inter-hemispheric competition and add support to a growing body of evidence that heightened excitability of the contralesional M1 may be adaptive rather than maladaptive in more severely impaired patients. The potential utility of biomarkers such as GABA concentration and upper limb spasticity to help identify suitable patients for contralesional tDCS warrants further investigation.

As expected, a-tDCS increased corticomotor excitability within the contralesional M1 evident by an increase in cMEP size in the non-paretic ECR. There was a trend for improved intralimb coordination during a-tDCS with the paretic arm and no change with the non-paretic arm. In patients with paretic cMEPs, a-tDCS increased corticomotor excitability in the ipsilesional 'non-stimulated' M1. Increased corticomotor excitability of the ipsilesional M1 could have arisen from tDCS-induced changes in transcallosal excitability from the contralesional to ipsilesional M1, and/or changes mediated at a subcortical level. As this is the first study to examine the neurophysiological effects of contralesional a-tDCS this requires further investigation.

The extent to which paretic upper limb circling performance improved after a-tDCS was not associated with the extent to which paretic cMEPs increased after a-tDCS. Therefore,

a-tDCS effects on neuronal excitability may have extended beyond the contralateral corticospinal pathway, to modulate task performance. For example, moderate-to-severely impaired patients exhibit an increased reliance on contralesional motor output (Bradnam et al., 2013, Jones et al., 2015). Facilitation of contralesional M1 pathways may have interacted with the effects of tDCS on ipsilesional M1 pathways and contributed to the trend towards better intralimb coordination after contralesional a-tDCS. Trends such as reduced propriospinal inhibition in the late component of cutaneous-induced suppression and increased ipsilateral MEP size lend support to the idea that a-tDCS increased both crossed and uncrossed motor pathway excitability. These effects may have been mediated via cortico-reticular projections onto cervical propriospinal neurons innervating the upper limb. After stroke, less propriospinal inhibition in the component correlates with better upper limb recovery (Mazevet et al., 2003) however the relationship between upper limb recovery and the late cortical component is unknown. Because only a limited number of patients produced reliable iMEPs and propriospinal-mediated EMG suppression, the effect of tDCS on motor pathways from the contralesional M1 warrants further examination.

Contrary to our hypothesis, contralesional c-tDCS did not affect corticomotor excitability or motor function. In a previous study of chronic stroke patients, contralesional c-tDCS suppressed contralesional M1 excitability (Bradnam et al., 2012) and degraded motor performance in patients with moderate-to-severe impairment (Bradnam et al., 2012, Yao et al., 2015). The difference between the present and previous findings may be related to differences in severity of impairment, timing of tDCS relative to the motor task, or other factors. In the present study, circle drawing was initiated during c-tDCS in patients with moderate-severe impairments whereas previously c-tDCS was delivered at rest and motor tasks performed post stimulation (Yao et al., 2015) in patients with mild-moderate impairments (Bradnam et al., 2012). In another study, contralesional a-tDCS delivered at rest

did not improve or worsen reaching performance with the paretic upper limb (Yao et al., 2015). Concurrent motor activity with tDCS possibly negated the suppressive effect of c-tDCS (Reis et al., 2009a, Stagg et al., 2011b, Stagg et al., 2011c), whereas concurrent task activity with a-tDCS may have enhanced the potential for positive behavioural effects (Reis et al., 2009b, Stagg et al., 2011b, Stagg et al., 2011c, Bikson et al., 2013). Delivering a-tDCS concurrently with task activity may preferentially modulate motor networks, thereby permitting tDCS to be somewhat functionally specific to neural substrates activated by the task (Bikson et al., 2013). When tDCS is delivered concurrently with motor training, positive effects may also be generalised, and transfer to untrained motor tasks (Waters-Metenier et al., 2014, Lefebvre et al., 2015). The generalisation of after-effects to other motor tasks is important for neurorehabilitation with the ultimate goal being to improve activities of daily living and quality of life.

Stroke rehabilitation urgently requires biomarkers to allow therapies to be selected and tailored to patient subgroups. In the present study, potential biomarkers were identified for selecting candidate stroke patients that are likely to benefit from contralesional anodal or cathodal tDCS. Spasticity has previously been shown to determine the effects of contralesional c-tDCS, whereby c-tDCS improved upper limb function in those with a MAS score of ≤ 1, but c-tDCS degraded upper limb function in those with a score of > 1 (Bradnam et al., 2012). In the present study, there was a trend for a positive relationship between intralimb coordination and spasticity, whereby patients with a high level of spasticity were positively affected by contralesional a-tDCS. As such, the MAS may represent a simple and salient biomarker to help determine the appropriate tDCS protocol for a given patient.

Previous studies using MRS have demonstrated the ipsilesional concentration of GABA may play a role in post stroke recovery (O'Shea et al., 2014, Blicher et al., 2015). In the present study, the detrimental effect of contralesional c-tDCS was associated with higher basal GABA concentrations in the ipsilesional M1. A higher ipsilesional GABA concentration could be indicative of poorer recovery, as a functional decrease of GABA-ergic inhibition would likely support motor learning and recovery (Lazar et al., 2010, Blicher et al., 2015). Both clinical and neurochemical biomarkers seem capable of identifying candidate stroke patients who may benefit from contralesional tDCS. Furthermore, the extent of interhemispheric imbalance prior to tDCS could also be a potential factor which mediates the after-effects of tDCS. The use of these and other potential biomarkers will be necessary when designing large interventional randomised controlled trials designed to improve outcomes in stroke rehabilitation.

The present study is a proof-of-concept that tDCS offers potential for up-regulating activity within the contralesional hemisphere of chronic stroke patients, which may be benefical for those with more severe impairment. A serious limitation of our study is the small sample size. Another limitation of the present study is that baseline data were not collected for all dependant measures in an effort to reduce time and patient fatigue. Instead some measures were compared between real and sham tDCS sessions. As such, we cannot fully discount that some findings may have reflected baseline differences between sessions. These limitations notwithstanding, the behavioural and neurophysiological findings support further investigation of approaches which may up-regulate contralesional excitability for a suitable cohort of chronic stroke patients. These finding challenge the interhemispheric imbalance model of stroke recovery, reminding us again that tDCS is not a ‘one size fits all’ intervention.

Acknowledgements

The authors would like to thank Ronan Mooney, Dr Clare Turner, Dr Victor Borges, and the Centre for Advanced MRI for their assistance. This research was supported by funding from Health Research Council of New Zealand project grant 14/136. AM was funded by a Health Research Council of New Zealand scholarship.

Conflict of interest

The authors declare no potential conflicts of interest.

Table 1. Patient characteristics.

Figure 1. Overview of study protocol. Session 1, clinical assessments. FM, Fugl-Meyer; ARAT, Action Research Arm Test; MAS, modified Ashworth spasticity scale. Session 2 – 4 participants underwent anodal, cathodal, or sham tDCS in separate sessions with the 'target' electrode positioned over the contralesional M1 (C) and 'reference' electrode on the ipsilesional (I) forehead. NP, non-paretic side; P, paretic side (grey arm); P+, cMEP positive; cMEPs, contralateral MEP; EMGsup, EMG suppression; iMEPs, ipsilateral MEP. Session 5 was to obtain MRI. Anatomical images are shown in scanner anatomical space, diffusion weighted imaging (DWI, left example image) and magnetic resonance spectroscopy (MRS, right example image and spectrum) optimised for GABA were collected. DWI was used to calculate the asymmetry index (FA_{AI}) between left and right posterior limbs of the internal capsule (PLIC, blue). MRS was obtained from voxels positioned over the left and right hand knob, and visual cortex (not shown). The GABA-optimised spectrum shows characteristic peaks for GABA and NAA from the M1 of a representative subject.

Figure 2. Anatomical T1-weighted images in the transverse plane are shown at the level of the lesion for each patient. Lesions are indicated by arrows. Patient numbers correspond with Table 1.

Figure 3. Neurophysiological effects of tDCS. A. In the non-paretic arm, contralateral MEPs (cMEP) were facilitated by a-tDCS and differed from sham (n=10). B. In the paretic arm, cMEPs after a-tDCS were different to sham (n=6). C. Ipsilateral MEPs (iMEP) showed a trend towards increased size after a-tDCS relative to sham (n=8). D-E. Cutaneous-induced EMG suppression calculated as 1-(C/NC) x 100. In the non-paretic arm, suppression was present in all sessions for the early and late component (n=10) but not in the paretic arm (n=4). E. In the late component of the paretic arm, suppression was reduced after a-tDCS compared to sham. The effects on propriospinal excitability are indicated by § to reflect the reduced sample size. The lower boundary refers to 25th percentile, horizontal line refers to median, upper boundary refers to 75th percentile. Error bars indicate 10th and 90th percentiles. Dashed line refers to pre tDCS (A, B) or sham tDCS (C). (*P<0.05, #P<0.1).

Figure 4. Confirmatory findings. A. The fractional anisotropy asymmetry index (FA_{AI}) was negatively associated with upper-limb Fugl-Meyer (UL-FM) score. Patients with larger asymmetry had worse impairment. cMEP positive patients (squares) were less impaired and had less asymmetry than cMEP negative patients (triangles). B-C. The transformed aspect ratio (AR) during sham tDCS was positively associated the action research arm test (ARAT) and UL-FM scores recorded at baseline.

Figure 5. Behavioural effects of anodal (A, B) and cathodal (A, C) tDCS on the aspect ratio (AR) with the paretic arm. A. Group average of ΔAR in the paretic arm at $post_1$ and $post_2$ separately and combined ($post_{1\&2}$). The lower boundary refers to 25th percentile, horizontal line refers to median, upper boundary refers to 75th percentile. Error bars indicate 10th and 90th percentiles. (#P<0.1). B. Anodal tDCS showed a trend for an association with patients' spasticity (MAS, modified Ashworth spasticity scale). Patients with worse spasticity made the most improvement after a-tDCS. C. Cathodal tDCS was associated with GABA:Cr in the ipsilesional M1. Open circle shows the excluded case. Patients with higher GABA concentrations were worsened by c-tDCS.

References

Ackerley SJ, Stinear CM. Stimulating stimulation: can we improve motor recovery following stroke using repetitive transcranial magnetic stimulation? Phys Ther Rev. 2010;15:302-8.

Bikson M, Rahman A. Origins of specificity during tDCS: anatomical, activity-selective, and input-bias mechanisms. Front Hum Neurosci. 2013;7:688.

Blicher JU, Near J, Naess-Schmidt E, Stagg CJ, Johansen-Berg H, Nielsen JF, et al. GABA levels are decreased after stroke and GABA changes during rehabilitation correlate with motor improvement. Neurorehabil Neural Repair. 2015;29:278-86.

Bradnam LV, Stinear CM, Barber PA, Byblow WD. Contralesional hemisphere control of the proximal paretic upper limb following stroke. Cereb Cortex. 2012;22:2662-71.

Bradnam LV, Stinear CM, Byblow WD. Cathodal transcranial direct current stimulation suppresses ipsilateral projections to presumed propriospinal neurons of the proximal upper limb. J Neurophysiol. 2011;105:2582-9.

Bradnam LV, Stinear CM, Byblow WD. Ipsilateral motor pathways after stroke: implications for non-invasive brain stimulation. Front Hum Neurosci. 2013;7:184.

Di Pino G, Pellegrino G, Assenza G, Capone F, Ferreri F, Formica D, et al. Modulation of brain plasticity in stroke: a novel model for neurorehabilitation. Nat Rev Neurol. 2014;10:597-608.

Dipietro L, Krebs HI, Fasoli SE, Volpe BT, Stein J, Bever C, et al. Changing motor synergies in chronic stroke. J Neurophysiol. 2007;98:757-68.

Gerloff C, Bushara K, Sailer A, Wassermann EM, Chen R, Matsuoka T, et al. Multimodal imaging of brain reorganization in motor areas of the contralesional hemisphere of well recovered patients after capsular stroke. Brain. 2006;129:791-808.

Jacobson L, Koslowsky M, Lavidor M. tDCS polarity effects in motor and cognitive domains: a meta-analytical review. Exp Brain Res. 2012;216:1-10.

Johansen-Berg H, Rushworth MF, Bogdanovic MD, Kischka U, Wimalaratna S, Matthews PM. The role of ipsilateral premotor cortex in hand movement after stroke. Proc Natl Acad Sci U S A. 2002;99:14518-23.

Jones TA, Adkins DL. Motor System Reorganization After Stroke: Stimulating and Training Toward Perfection. Physiology. 2015;30:358-70.

Kang N, Summers JJ, Cauraugh JH. Transcranial direct current stimulation facilitates motor learning post-stroke: a systematic review and meta-analysis. J Neurol Neurosurg Psychiatry. 2015;87:345-55.

Krabben T, Molier BI, Houwink A, Rietman JS, Buurke JH, Prange GB. Circle drawing as evaluative movement task in stroke rehabilitation: an explorative study. J Neuroeng Rehabil. 2011a;8:15.

Krabben T, Prange GB, Molier BI, Rietman JS, Buurke JH. Objective measurement of synergistic movement patterns of the upper extremity following stroke: an explorative study. IEEE Int Conf Rehabil Robot. 2011b;2011:5975430.

Lazar RM, Berman MF, Festa JR, Geller AE, Matejovsky TG, Marshall RS. GABAergic but not anti-cholinergic agents re-induce clinical deficits after stroke. J Neurol Sci. 2010;292:72-6.

Lefebvre S, Dricot L, Laloux P, Gradkowski W, Desfontaines P, Evrard F, et al. Neural substrates underlying stimulation-enhanced motor skill learning after stroke. Brain. 2015;138:149-63.

Lotze M, Beutling W, Loibl M, Domin M, Platz T, Schminke U, et al. Contralesional motor cortex activation depends on ipsilesional corticospinal tract integrity in well-recovered subcortical stroke patients. Neurorehabil Neural Repair. 2012;26:594-603.

Lotze M, Markert J, Sauseng P, Hoppe J, Plewnia C, Gerloff C. The role of multiple contralesional motor areas for complex hand movements after internal capsular lesion. J Neurosci. 2006;26:6096-102.

Mardia KV, Zemroch PJ. Circular Statistics. J Roy Stat Soc B. 1975;24:147-50.

Mazevet D, Meunier S, Pradat-Diehl P, Marchand-Pauvert V, Pierrot-Deseilligny E. Changes in propriospinally mediated excitation of upper limb motoneurons in stroke patients. Brain. 2003;126:988-1000.

McCambridge AB, Stinear JW, Byblow WD. A dissociation between propriospinal facilitation and inhibition after bilateral transcranial direct current stimulation. J Neurophysiol. 2014;111:2187-95.

Mescher M, Merkle H, Kirsch J, Garwood M, Gruetter R. Simultaneous in vivo spectral editing and water suppression. NMR Biomed. 1998;11:266-72.

Nowak DA, Grefkes C, Ameli M, Fink GR. Interhemispheric Competition After Stroke: Brain Stimulation to Enhance Recovery of Function of the Affected Hand. Neurorehabil Neural Repair. 2009;23:641-56.

O'Shea J, Boudrias MH, Stagg CJ, Bachtiar V, Kischka U, Blicher JU, et al. Predicting behavioural response to TDCS in chronic motor stroke. Neuroimage. 2014;85:924-33.

Plow EB, Sankarasubramanian V, Cunningham DA, Potter-Baker K, Varnerin N, Cohen LG, et al. Models to Tailor Brain Stimulation Therapies in Stroke. Neural Plast. 2016;2016:4071620.

Reis J, Schambra HM, Cohen LG, Buch ER, Fritsch B, Zarahn E, et al. Noninvasive cortical stimulation enhances motor skill acquisition over multiple days through an effect on consolidation. Proc Natl Acad Sci U S A. 2009a;106:1590-5.

Reis J, Schambra HM, Cohen LG, Buch ER, Fritsch B, Zarahn E, et al. Noninvasive cortical stimulation enhances motor skill acquisition over multiple days through an effect on consolidation. Proc Natl Acad Sci U S A. 2009b;106:1590-5.

Smith SM. Fast robust automated brain extraction. Hum Brain Mapp. 2002;17:143-55.

Stagg CJ, Bachtiar V, Johansen-Berg H. The role of GABA in human motor learning. Curr Biol. 2011a;21:480-4.

Stagg CJ, Jayaram G, Pastor D, Kincses ZT, Matthews PM, Johansen-Berg H. Polarity and timing-dependent effects of transcranial direct current stimulation in explicit motor learning. Neuropsychologia. 2011b;49:800-4.

Stagg CJ, Nitsche MA. Physiological basis of transcranial direct current stimulation. Neuroscientist. 2011c;17:37-53.

Vanhamme L, Sundin T, Hecke PV, Huffel SV. MR spectroscopy quantitation: a review of time-domain methods. NMR Biomed. 2001;14:233-46.

Walters MR, Carson RG. A method for calculating the circularity of movement trajectories. J Mot Behav. 1997;29:72-84.

Ward NS, Brown MM, Thompson AJ, Frackowiak RS. Neural correlates of motor recovery after stroke: a longitudinal fMRI study. Brain. 2003;126:2476-96.

Waters-Metenier S, Husain M, Wiestler T, Diedrichsen J. Bihemispheric transcranial direct current stimulation enhances effector-independent representations of motor synergy and sequence learning. J Neurosci. 2014;34:1037-50.

Yao J, Drogos J, Veltink F, Anderson C, Concha Urday Zaa J, Hanson LI, et al. The effect of transcranial direct current stimulation on the expression of the flexor synergy in the paretic arm in chronic stroke is dependent on shoulder abduction loading. Front Hum Neurosci. 2015;9:262.

Yousry TA, Schmid UD, Alkadhi H, Schmidt D, Peraud A, Buettner A, et al. Localization of the motor hand area to a knob on the precentral gyrus. A new landmark. Brain. 1997;120:141-57.

Zhang Y, Brady M, Smith S. Segmentation of brain MR images through a hidden Markov random field model and the expectation-maximization algorithm. IEEE Trans Med Imaging. 2001;20:45-57.

Ziemann U, Ishii K, Borgheresi A, Yaseen Z, Battaglia F, Hallett M, et al. Dissociation of the pathways mediating ipsilateral and contralateral motor-evoked potentials in human hand and arm muscles. J Physiol. 1999;518:895-906.

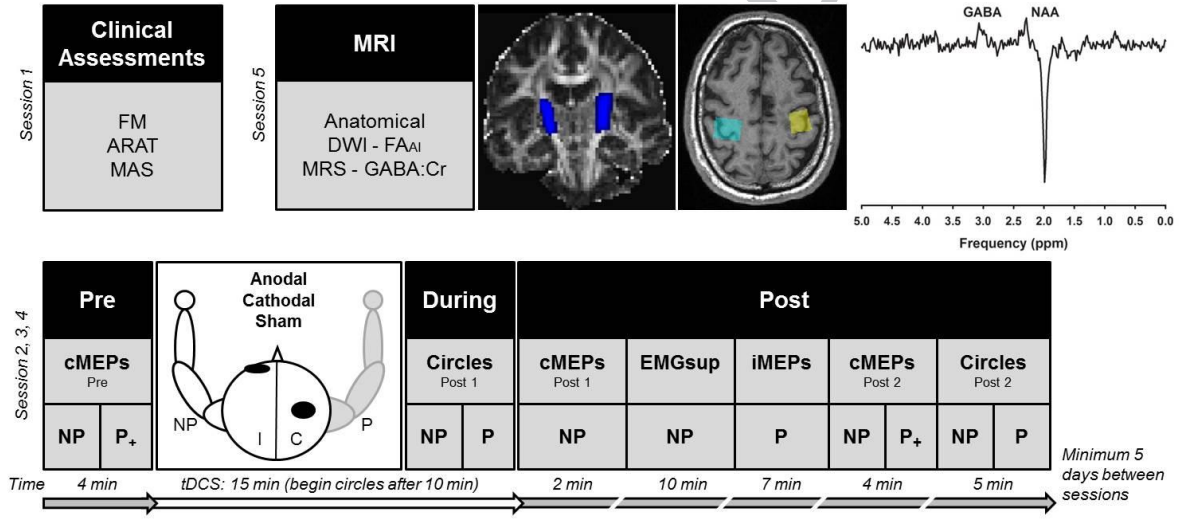

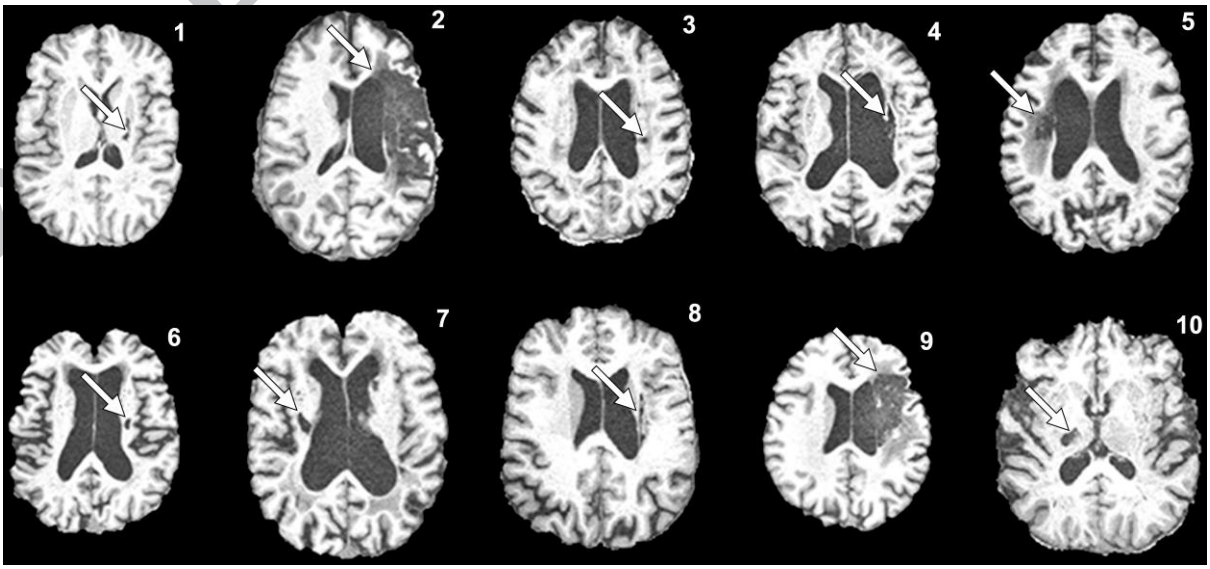

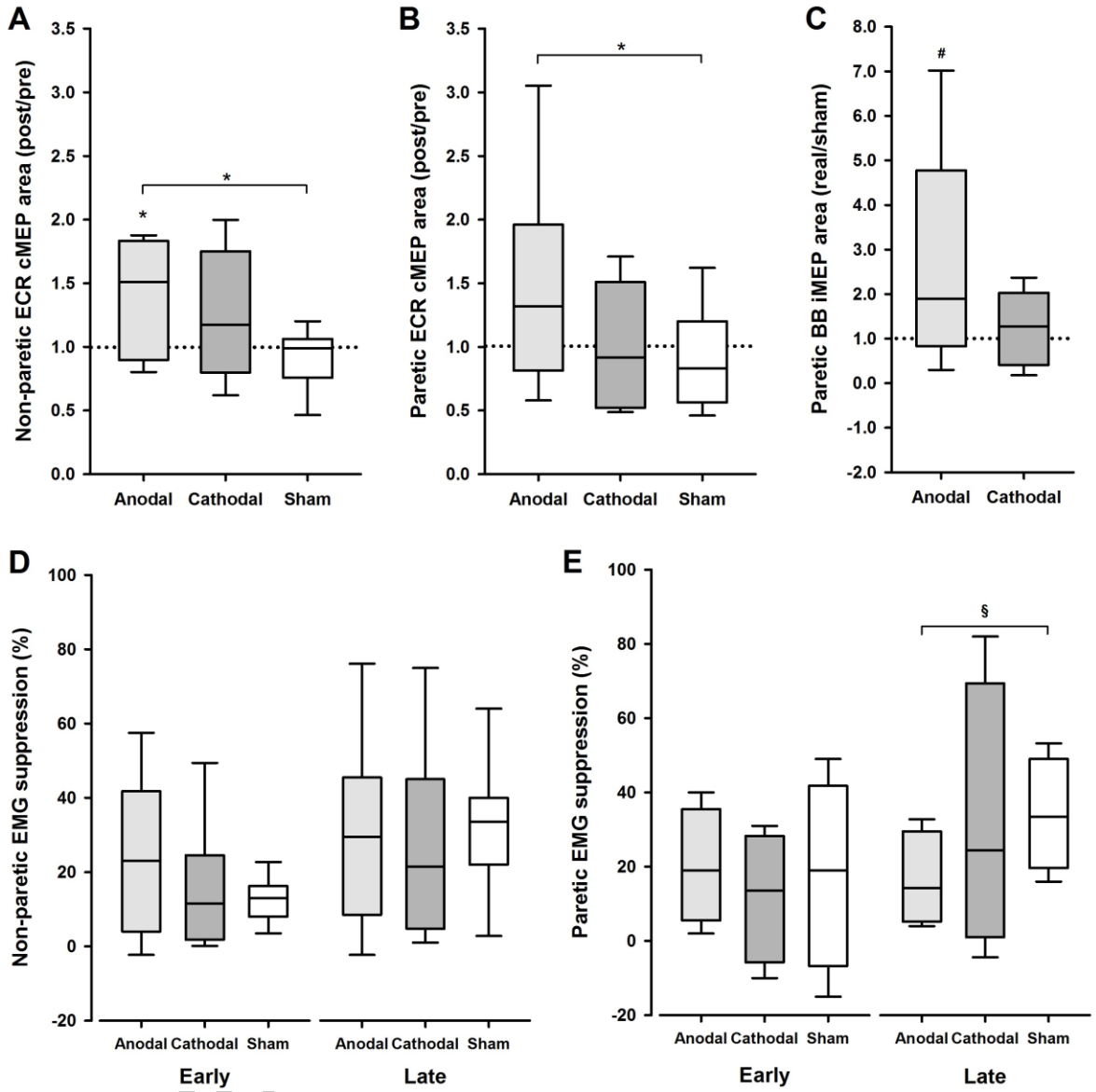

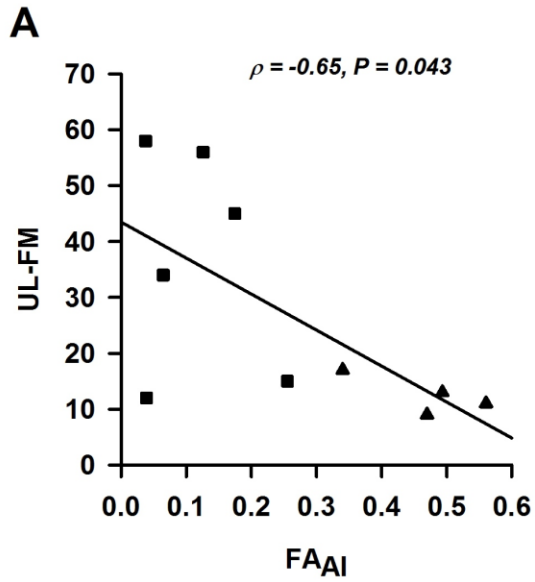

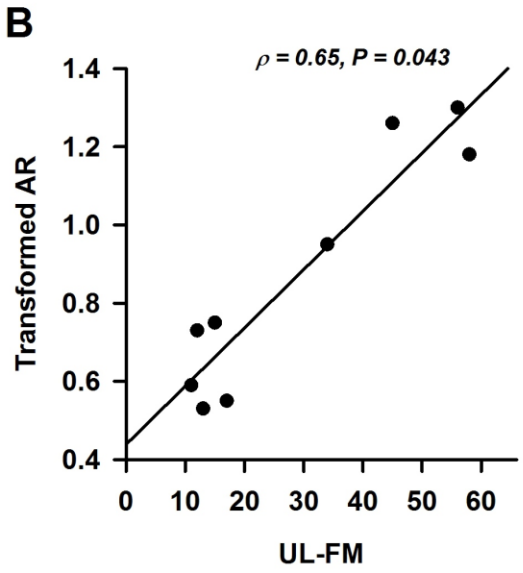

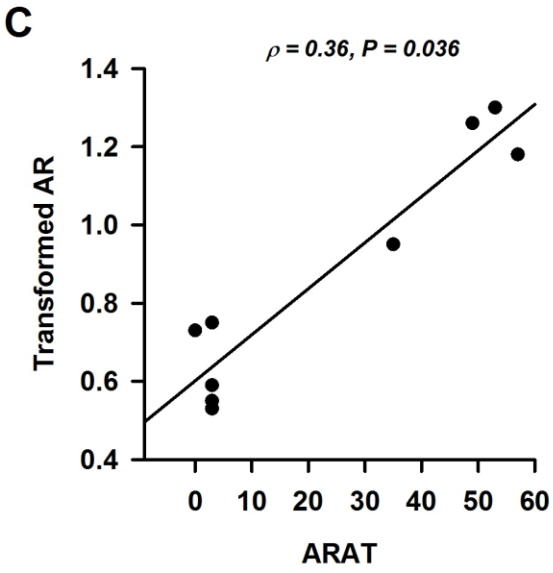

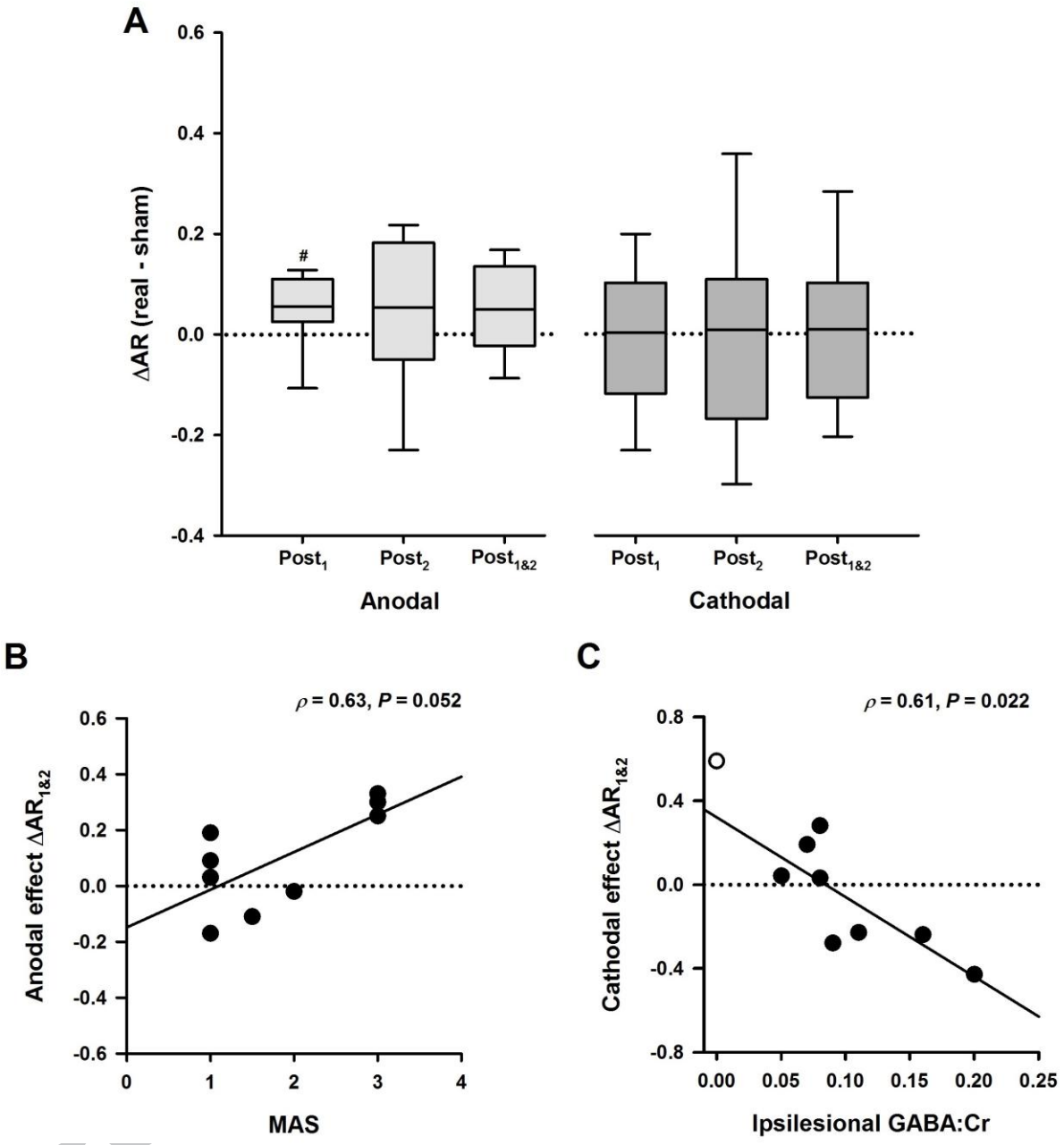

Subject	Age (yrs)	Gender	Months post stroke	Paretic limb	UL-FM	ARAT	MAS	FA_{AI}	cMEP	iME
1	65	M	84	L	34	35	2	0.06	+	+
2	62	F	192	L	13	3	1+	0.49	-	+
3	72	M	108	R	58	57	1	0.04	+	+
4	66	M	180	L	11	3	3	0.56	-	+
5	75	M	108	R	15	3	3	0.26	+	+
6	80	M	48	L	45	49	1	0.17	+	+
7	74	M	144	R	12	0	3	0.04	+	+
8	72	F	84	L	9	0	3	0.34	-	-
9	58	M	168	L	17	3	1	0.47	-	-
10	74	M	14	R	56	53	1	0.13	+	+
Mean	**69.8**	**8M/2F**	**113**	**4R/6L**	**27**	**20.6**	**1.95**	**0.26**	**6+/4-**	**8+/**
Max	**80**		**192**		**58**	**57**	**3**	**0.56**		
Min	**58**		**14**		**9**	**0**	**1**	**0.04**		

Note: UL-FM, Fugl-Meyer upper limb score (maximum 66); ARAT, action research arm test (maximum 57); MAS, modified Ashworth spasticity scale for the elbow (maximum 4). FAAI, fractional anisotropy asymmetry index (perfect symmetry=0) within the posterior limb of the internal capsule (PLIC). Presence (+) or absence (-) of contralateral or ipsilateral motor evoked potentials (cMEP, iMEP) in the paretic arm